WATER RESOURCES RESEARCH, VOL. 37, NO. 10, PAGES 2631–2636, OCTOBER 2001

Water retention of prefractal porous media generated with the homogeneous and heterogeneous algorithms

Michael C. Sukop[1]

Department of Agronomy and Center for Computational Sciences, University of Kentucky Lexington, Kentucky, USA

Edmund Perfect[2]

Department of Agronomy, University of Kentucky, Lexington, Kentucky, USA

Nigel R. A. Bird

Silsoe Research Institute, Silsoe, Bedford, England, UK

Abstract. Fractal models of porous media are of interest in numerous scientific disciplines, including hydrology and soil science. This interest arises in part from the ability of these models to parsimoniously produce highly complex and richly structured geometries. Examination of the soil hydrology literature suggests that there are at least two different ways these models are being constructed. We review the two primary algorithms and compare the computed water retention behavior of the different media. Water retention is computed using a method that explicitly considers the connections between pores and to the atmosphere. The distributions of simulated water saturations (for 1000 realizations) around their median values as a function of applied tension were complex and multimodal for both homogeneous and heterogeneous prefractals. The range between the first and third quartiles for the water retention in heterogeneous prefractal structures was, on average, more than twice as large as that for the homogeneous prefractals. This suggests that relations between fractal parameters used to construct the porous media and the water retention behavior of the media can be more readily determined for homogeneous prefractals.

1. Introduction

Fractal models of porous media are enjoying considerable popularity [e.g., *Adler and Thovert*, 1993; *Perrier et al*., 1995; *Bird and Dexter*, 1997; *Rieu and Perrier*, 1998; *Perrier et al*., 1999; *Rappoldt and Crawford*, 1999]. This is due in part to the relatively small number of parameters that can define a random fractal porous medium of great complexity and rich structure. Also, fractal scaling of natural porous media has been widely anticipated on the basis of the observed power law form of soil water retention curves [*Ahl and Niemeyer*, 1989; *Tyler and Wheatcraft*, 1990; *Rieu and Sposito*, 1991a, 1991b, 1991c; *Perrier et al*., 1996; *Perfect*, 1999]. There has been considerable debate about the validity of the approaches presented in these papers because they generally neglect pore connectivity [*Bird et al*., 1996; *Rieu and Perrier*, 1998]. One way that this limitation can be surmounted is to compute retention in simulated realizations of known fractal porous media using a method that explicitly accounts for pore connectivity [*Perrier et al*., 1995; *Bird and Dexter*, 1997; *Stepanek et al*., 1999]. As these and other types of simulations in fractal porous media become more widespread, it is valuable to examine the methods used to generate the media and their properties.

Various modifications of basic fractal-generating algorithms, such as assemblages of fractal "patches" or fractal cell arrays [*Bird and Dexter*, 1997; *Rappoldt and Crawford*, 1999] and pore-solid fractals [*Perrier et al*., 1999] have been proposed and applied. Our focus is on the most basic models, however, and we do not address these variants further. *Rieu and Perrier* [1998] make the distinction between "mass" and "pore" fractal models. Only mass fractal models are considered here, though the issues addressed apply equally to random pore fractal models. We review fundamental fractal scaling requirements and contrast different fractal-generating algorithms in terms of their water retention behavior.

2. Basic Prefractal Porous Media

The fractals we consider first are scale-invariant constructions that follow simple number-size relations. Conceptually, porous fractals are often constructed from a solid starting mass by an iterative process of mass removal and rescaling. As a concrete example, we consider the perhaps familiar Sierpinski carpet, which has $E = 2$ (the embedding or Euclidian dimension), $b = 3$ (a scale invariance factor), and $p = 8/9$ (the probability of a solid at any iteration) (Figure 1a).

Construction begins with a solid square of size 1×1 from which one square area of size 1/3 by 1/3 is removed from the center. $N(r)$ is the number of solids of the new size remaining at any iteration (for our example, $N(r) = 8$ for the first

[1]Now at Department of Plants, Soils, and Biometeorology, Utah State University, Logan, Utah, USA.

[2]Now at Department of Geological Sciences, University of Tennessee, Knoxville, Tennessee, USA.

Paper number 2000WR000097.
0043-1397/01/2000WR000097$09.00

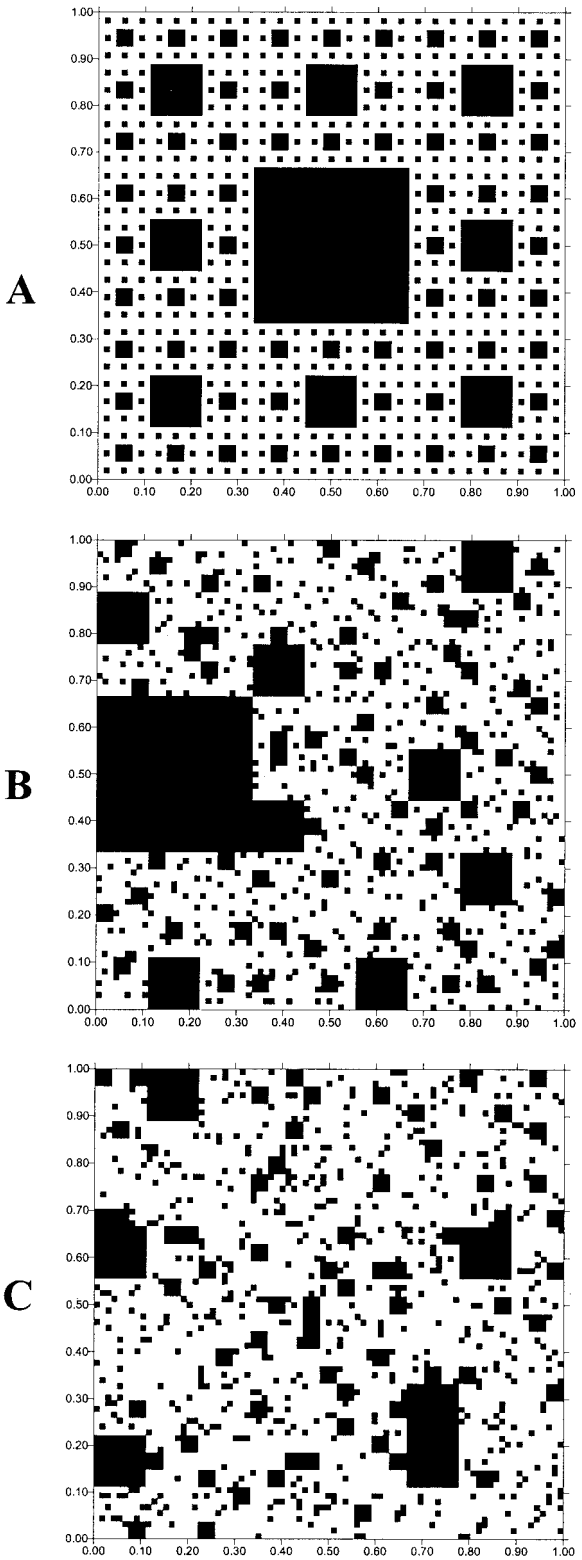

Figure 1. (a) Sierpinski carpet constructed to fourth iteration (solids indicated by white; voids indicated by black). (b) Randomized Sierpinski carpet constructed to fourth iteration with the homogeneous algorithm. Note that the number of pores of each size class (neglecting coalescence) is in strict agreement with the number in the standard Sierpinski carpet (Figure 1a). (c) Randomized Sierpinski carpet constructed to fourth iteration with the heterogeneous algorithm. Note that the number of pores of each size class does not agree with the number in the standard Sierpinski carpet (Figure 1a) or the randomized carpet in Figure 1b.

iteration), and r is the linear measure of a pore or solid. Note that r depends on b as $r = (1/b)^i$, where i is the iteration. In a fractal of unit side length, $N(r) = r^{-D}$, and the ratio $-\log N(r)/\log r$ gives the mass fractal dimension D. As is generally true for such ratios, point estimates based on individual pairs of $N(r)$ and r or slope estimates based on numerous pairs can be computed. For the standard Sierpinski carpet, $N(r) = 8$ and $r = 1/3$ at the first iteration. Hence on the basis of this pair of $N(r)$ and r, $D = -\log(8)/\log(1/3) = 1.89\ldots$. At the second iteration, $N(r) = 64$ and $r = 1/9$. Therefore $D = -\log(64)/\log(1/9) = 1.89\ldots$. Computation of the double logarithmic slope between the points leads to

$$D = -\frac{d \log N}{d \log r}$$

$$= -\frac{\Delta \log N}{\Delta \log r} = -\frac{\log 8 - \log 64}{\log 1/3 - \log 1/9} = 1.89\ldots. \quad (1)$$

We recover the exact fractal dimension from either procedure.

The porosity (ϕ) of a "true" fractal (in which the generating process is iterated an infinite number of times) is always unity. Hence such models are of little use as models of natural porous media such as soil, aquifer, or reservoir material. However, by introducing a lower "cutoff" size, where the generating process ceases, we can maintain a realistic porosity. Thus we can define such a "prefractal" [*Feder*, 1988], in which the generating process is iterated only i times, in terms of any three of the following four parameters: D, b, i, and ϕ (or p). The water retention model of *Perfect* [1999] describes the drainage of such a prefractal when a number of assumptions are met. The model incorporates a tension at dryness (ψ_d) that relates to the iteration i of the fractal. The model can be written as

$$S = \frac{\psi^{D-E} - \psi_d^{D-E}}{\psi_e^{D-E} - \psi_d^{D-E}}, \quad (2)$$

where S is the relative saturation, ψ is the tension of interest, ψ_e is the air entry tension, and ψ_d is the tension at dryness.

3. Algorithms for Generating Randomized Prefractal Porous Media

3.1. Homogeneous Algorithm

Clearly, the prefractal in Figure 1a bears little resemblance to natural porous media like soils and aquifer or reservoir materials because of its regularity and lack of pore connectivity. Now the question arises, How are we to construct a randomized version of a prefractal? One method that maintains strict adherence to the fractal scaling law $N(r) = r^{-D}$, and therefore returns the correct fractal dimension using both the individual point ratios $\log(N(r))/\log(1/r)$ and the slope measures, is to assign a random permutation of the integers 1 through b^E to each site of a lattice and then retain only those with an integer value $j \leq pb^E$ as solids. Iterating this algorithm produces prefractal porous media that can be classified as homogeneous [*Gouyet*, 1996]. This approach has also been called "constrained curdling" [*Mandelbrot*, 1983].

For the classical Sierpinski carpet, $1 \leq j \leq 9$, $p = 8/9$, $b = 3$, and $E = 2$. Hence sites with $j \leq 8/9 \times 3^2$ (i.e., $j \leq 8$) are retained as solids. For the second iteration the same algorithm is applied independently to each of the eight solids that remain and so on for subsequent iterations. Figure 1b shows the re-

Table 1. Nine Realizations of Nine Random Numbers in [0, 1][a]

Realization	Random Numbers in [0, 1]									*N*
1	0.8712	0.606	0.2482	0.4722	0.566	(0.9357)	0.3504	(0.9946)	0.0136	7
2	0.5845	0.8111	(0.9886)	0.7324	0.7607	0.6739	0.613	0.8774	0.7895	8
3	0.6026	0.4618	0.5643	(0.9806)	0.3452	0.4279	0.3377	0.6259	(0.8996)	7
4	0.4882	0.0937	0.2205	0.6668	0.4475	0.8328	0.636	0.2119	0.0022	9
5	(0.9426)	0.1027	0.8775	0.6831	0.5158	0.1713	0.5166	(0.9155)	0.5163	7
6	0.3465	0.8745	0.7276	0.8754	0.1573	0.4406	0.5195	0.1343	0.6244	9
7	0.1997	0.0608	0.8531	0.5077	(0.9809)	0.7524	0.6264	(0.9681)	0.2652	7
8	0.0981	0.8472	0.1777	0.4679	0.2988	0.6155	(0.9492)	0.6199	0.399	8
9	0.6521	0.4541	0.5403	0.2448	0.1546	0.2542	0.2235	0.6408	(0.9776)	8

[a]Values greater than $p = 8/9$ (pores) are in parentheses. N denotes the number of solids created by the heterogeneous algorithm.

sults of the application of this algorithm. If we neglect the coalescence of adjacent pores, there is exactly one large pore (and hence eight solids) at the first iteration, and there are exactly eight new pores at the second iteration. Pore coalescence does not affect the total porosity but may be of significance in the study of water retention.

3.2. Heterogeneous Algorithm

Bird and Dexter [1997] and *Rappoldt and Crawford* [1999] present random prefractal models of porous media. In both cases some of these prefractals were constructed using an algorithm that can be summarized as follows: (1) Choose a probability p that a site is a solid. (2) For each site in a space divided into b^E sites, generate a uniformly distributed random number in the interval [0, 1]. (3) If the random number is greater than p, make the site a pore. Models generated with this algorithm can be classified as heterogeneous [*Gouyet*, 1996] as opposed to the homogeneous model we present in Figure 1b. *Mandelbrot* [1983] uses the term "canonical curdling" to describe this approach. The defining characteristic of a heterogeneous model is that $N(1/b)$ (the number of solids out of b^E possible choices each time the pore/solid assignment is made and henceforth simply N) is a random variable. Let us consider the behavior of this algorithm. Say that we wish to generate a randomized Sierpinski carpet. Hence $p = 8/9$ ($= 0.888\ldots$). We generate nine realizations of b^E ($=9$) random numbers and show them in Table 1. It is clear from Table 1 that this algorithm often fails to return the number of solids (eight for the Sierpinski carpet) needed to satisfy the simple fractal scaling law $N(r) = r^{-D}$. For the first realization on the first line, $N(r) = 7$ and $r = 1/3$. Hence the fractal dimension based on the point estimate is $D = -\log(7)/\log(1/3) = 1.77\ldots$ rather than $D = 1.89\ldots$ as is characteristic of the classical Sierpinski carpet (Figure 1a).

Figure 1c shows a randomized Sierpinski carpet based on the heterogeneous algorithm. In this realization, there are no pores at the first iteration (like realization 4 of Table 1) and only six (again ignoring pore coalescence) at the second level. The point estimates of the fractal dimension are 2.000, 1.965, 1.945, and 1.933 for the first, second, third, and fourth iterations, respectively. *Mandelbrot* [1983] defines the generalized similarity dimension for the heterogeneous case as $D^* = \log\langle N\rangle/\log(1/b)$, where $\langle N\rangle$ is the expectation of $N(1/b)$. If the algorithm does not yield the empty set, then the pointwise dimensions (i.e., $D = -\log N(1/b^i)/\log(1/b^i)$) tend to the limit D^* with increasing iteration of the fractal structure. For a homogeneous medium, there is a finite set of dimensions corresponding to the allowed rational values of p; whereas for the heterogeneous case, there is an infinite set. The slope estimate also tends to the limit D^* as the number of iterations increases. We obtain a slope estimate of 1.9096 after four iterations in comparison with the limiting value of $1.89\ldots$.

Prefractal structures generated with the homogeneous algorithm exhibit variable pore connectivity, but, for a given choice of p, they have a unique fractal dimension and, associated with this, a unique pore size distribution (ignoring pore coalescence) and porosity. The heterogeneous prefractal models display additional levels of complexity, with variable inferred fractal dimension, pore size distribution, and porosity. Consequently, the simulation of soil processes in these two models will exhibit differences reflecting the different levels of complexity. In particular, the simpler homogeneous algorithm generates model porous media that share a common pore size distribution and porosity. This offers an opportunity to isolate the impact of variable pore connectivity as a function of a uniquely defined fractal dimension.

4. Application to Water Retention

4.1. Previous Work and Method

In perhaps the first paper to explicitly consider the effects of pore connectivity on water retention in a prefractal model of porous media, *Bird and Dexter* [1997] computed moisture tension relations in two-dimensional prefractal pore networks. They simulated drainage in $b = 3$ and $i = 5$ randomized Sierpinski carpets by allowing three sides of the prefractal structure to be open to the atmosphere, while the bottom was connected to a water sink. At a given tension all pores of size greater than r that are filled with water and are connected to the atmosphere by at least one path consisting of pores no smaller than r drain. Note that this approach also neglects the coalescence of pores that can lead to pores larger than any particular size r computed from the fractal scaling equations. For example, consider the largest pore of Figure 1b, which is enlarged relative to the $1/3 \times 1/3$ size produced by the fractal-generating process because of its connection to other pores. The tension at which a pore drains completely is taken as inversely proportional to the size r, as it is in the Young-Laplace equation. This approach is therefore similar to most others in its assumption of purely capillary behavior. The approach is different from most others, however, in that it considers the pore connectivity.

4.2. Results

Bird and Dexter [1997] considered only heterogeneous prefractals in their work. Figure 2 compares water retention simulations on prefractal media generated with the homogeneous and heterogeneous algorithms at three different p values using

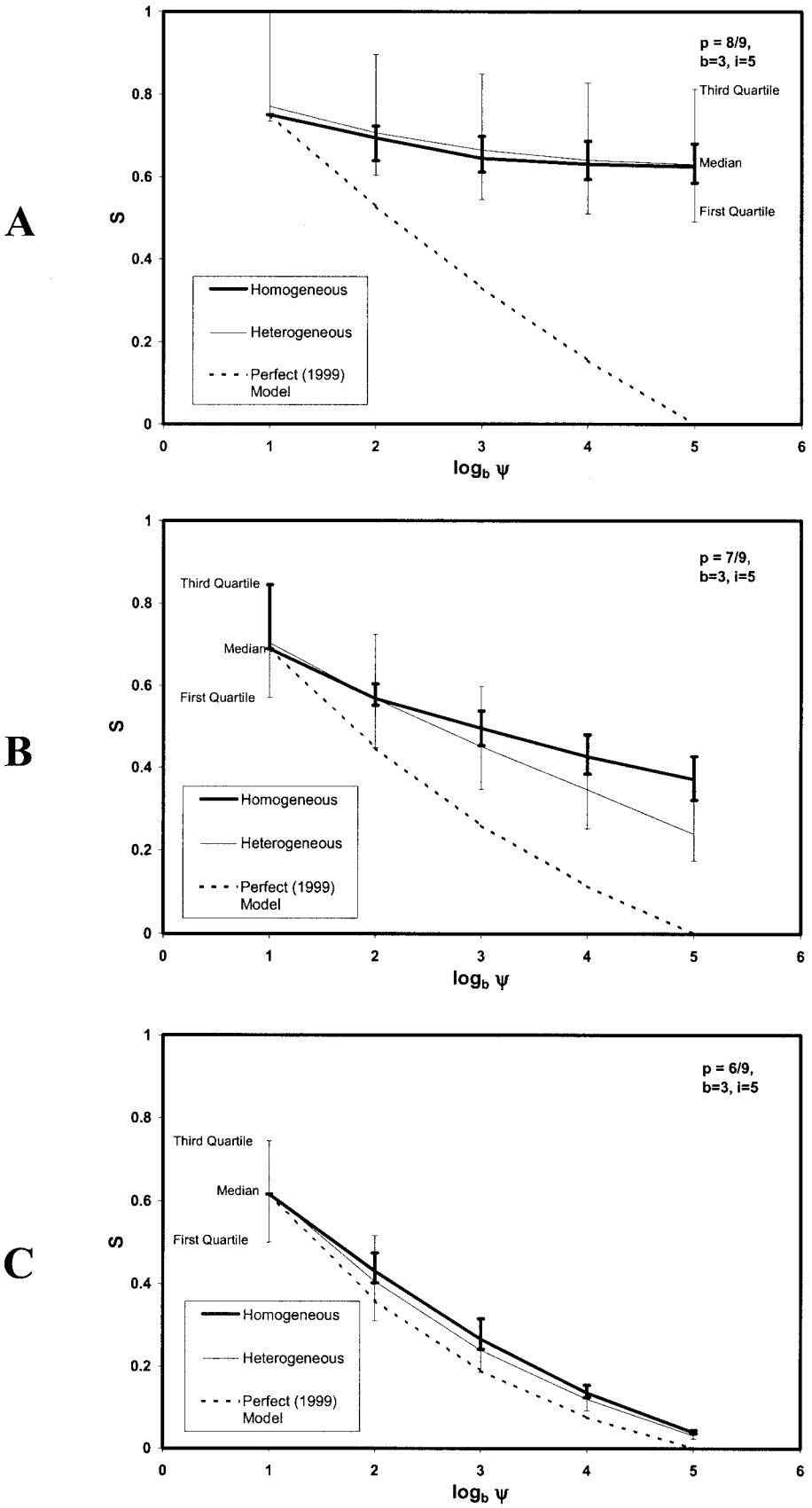

Figure 2. Impact of homogeneous and heterogeneous fractal-generating algorithms on simulated water retention for 1000 realizations of two-dimensional $b = 3$ and $i = 5$ prefractal porous media with different p values: (a) $p = 8/9$, (b) $p = 7/9$, and (c) $p = 6/9$.

Table 2. Ratio of Interquartile Ranges of Saturation for Heterogeneous and Homogeneous Algorithms at Each Tension for Varying p[a]

$\log_b \psi$	$p = 8/9$	$p = 7/9$	$p = 6/9$
1	∞[b]	1.76	∞[b]
2	3.52	5.33	2.90
3	3.53	2.98	1.75
4	3.43	2.33	2.01
5	3.39	1.58	1.96

[a]Difference between first and third quartiles for the heterogeneous case is divided by the difference between the first and third quartiles for the homogeneous case.
[b]Interquartile range of homogeneous results equals 0.

the method of *Bird and Dexter* [1997]. Here $\log_b \psi$ is the scaled log of tension. As noted in section 2, r depends on b as $r = (1/b)^i$, where i is the iteration. Because $\psi \propto 1/r \propto b^i$ in the Young-Laplace equation, taking logarithms yields $\log \psi \propto i \log b$ or $\log_b \psi \propto i$. Hence $\log_b \psi$ can be represented by the prefractal's iteration i. The p values, 6/9, 7/9, and 8/9, were selected to maintain a reasonable range of porosities. The porosity of a homogeneous prefractal is given by $1 - p^i$, but the porosity of a heterogeneous prefractal is not predictable a priori. After five iterations the homogeneous structure porosities ranged from 45 to 87%, while those from the heterogeneous algorithm ranged from 32 to 97%.

Figure 2 reveals an important distinction between the fractal algorithms; there is, in general, less variability in the computed drainage curves for the structures generated with the homogeneous algorithm. This must be the case because all homogeneous structures belong to a subset of the possible heterogeneous structures. The distributions of simulated water saturations around their median values as a function of applied tension were complex and multimodal for both homogeneous and heterogeneous prefractals. Therefore we use nonparametric statistics to summarize the results. These distributions reflect the complex connectivity conditions that arise in these porous media.

The principal findings are that the range of saturations between the first and third quartiles for water retention in heterogeneous prefractal structures was, on average, more than twice as large as that for homogeneous prefractals (Table 2). Thus the effects of pore connectivity on water retention for a particular set of prefractal parameters can be better elucidated by the less variable structures generated with the homogeneous algorithm.

The deviation in the median saturations for the homogeneous and heterogeneous algorithms when $p = 7/9$ (Figure 2b) may be explained by different degrees of pore interconnectedness in the prefractal media. The critical fractal dimension for sample-spanning pore percolation in homogeneous random prefractal porous media with $E = 2$, $b = 3$, and $i = 5$ is $D_c \approx 1.716$ [*Sukop et al.*, 2001]. Pore percolation occurs in these media when $D < D_c$. When $p = 8/9$ ($D = 1.89 \ldots$) both homogeneous and heterogeneous networks are poorly connected, and air has limited access to the pore system. Consequently, saturation remains high over all tensions. When $p = 6/9$ ($D = 1.63 \ldots$), both networks are sufficiently well connected to permit significant air invasion. For the intermediate case, $p = 7/9$ ($D = 1.77 \ldots$), drainage is always hindered in the homogeneous structures; whereas for the heterogeneous structures, a subset of the realizations have higher porosity and higher connectivity, offering routes for air invasion into the pore network.

Bird and Dexter [1997] conclude that within certain parameter ranges, pore connectivity can make it impossible to accurately measure the pore size distribution from the water retention curve. The algorithmic differences in assigning pores do not have a substantial impact on this conclusion.

Figure 2 also shows the predictions of the *Perfect* [1999] water retention model (equation (2)). At high p values the saturations computed considering pore connectivity differ significantly from those predicted by this model. The *Perfect* [1999] model is directly based on prefractal porous media of the type investigated in this note, except that complete pore connectivity (including a path of larger pores connecting any given pore to the atmosphere) and no coalescence of pores are assumed. Under those circumstances the air entry tension is always related to the size of the largest pores, and the tension at dryness is always related to the smallest pore size. The largest pore size is determined by the scaling factor b (for a carpet of unit side length it is $1/b$), and the smallest pore size is determined by the scaling factor and the iteration level i (it is $1/b^i$). Through the Young-Laplace equation the air entry tension and the tension at dryness are also completely determined by these parameters: $\psi_e \propto 1/b$ and $\psi_d \propto 1/b^i$. Taking logarithms and ignoring any constants yields $\log_b \psi_e = 1$ and $\log_b \psi_d = 5$ for the fifth iteration porous media under consideration in Figure 2.

Thus, if the assumptions of the *Perfect* [1999] model are met, ψ_d in (2) is determined by the smallest pore size. In randomized prefractal media, however, pore connectivity is usually incomplete, and dryness cannot be achieved at any tension if pores containing water are isolated. This is most significant when the connectivity of the pore network is low (i.e., when the fractal dimension of the medium is high and the porosity is low). Figure 2a shows that because of pore isolation, little and eventually no reduction in saturation occurs when tension is increased. The optimal ψ_d is therefore infinite. At lower p values (higher porosity, see Figure 2c) the Perfect model works significantly better.

5. Conclusions

We have demonstrated the increased variability in computed soil water retention that results from application of the heterogeneous algorithm as compared to results obtained with the homogeneous algorithm. The distributions of simulated water saturations around their median values as a function of applied tension were complex and multimodal for both homogeneous and heterogeneous prefractals. The range between the first and third quartiles for the water retention in heterogeneous prefractal structures was, on average, more than twice as large as that for the homogeneous prefractals. This suggests that the homogeneous algorithm may be superior when the goal is to test the effect of fractal dimension on processes occurring in the medium. Fitting the *Perfect* [1999] model to experimental water retention data does not necessarily yield an estimate of the mass fractal dimension of the underlying porous medium because of incomplete pore connectivity and an assumption of purely capillary behavior.

Acknowledgments. Partial funding for this work was provided by the University of Kentucky's Research Challenge Trust Fund and the University of Kentucky's Center for Computational Science.

References

Adler, P. M., and J.-F. Thovert, Fractal porous media, *Transp. Porous Media*, *13*, 41–78, 1993.

Ahl, C., and J. Niemeyer, The fractal dimension of the pore-volume inside soils, *Z. Pfanzenernaehr. Bodenkd.*, *152*, 457–458, 1989.

Bird, N. R. A., and A. R. Dexter, Simulation of soil water retention using random fractal networks, *Eur. J. Soil Sci.*, *48*, 633–641, 1997.

Bird, N. R. A., F. Bartoli, and A. R. Dexter, Water retention models for fractal soil structures, *Eur. J. Soil Sci.*, *47*, 1–6, 1996.

Feder, J., *Fractals*, 283 pp., Plenum, New York, 1988.

Gouyet, J.-F., *Physics and Fractal Structures*, translated from French, 234 pp., Springer-Verlag, New York, 1996.

Mandelbrot, B. B., *The Fractal Geometry of Nature*, updated and augmented ed., 468 pp., W. H. Freeman, New York, 1983.

Perfect, E., Estimating soil mass fractal dimensions from water retention curves, *Geoderma*, *88*, 221–231, 1999.

Perrier, E., C. Mullon, M. Rieu, and G. de Marsily, Computer construction of fractal soil structures: Simulation of their hydraulic and shrinkage properties, *Water Resour. Res.*, *31*, 2927–2943, 1995.

Perrier, E., M. Rieu, G. Sposito, and G. de Marsily, Models of the water retention curve for soils with a fractal pore size distribution, *Water Resour. Res.*, *32*, 3025–3031, 1996.

Perrier, E., N. Bird, and M. Rieu, Generalizing the fractal model of soil structure: The pore-solid fractal approach, *Geoderma*, *88*, 137–164, 1999.

Rappoldt, C., and J. W. Crawford, The distribution of anoxic volume in a fractal model of soil, *Geoderma*, *88*, 329–347, 1999.

Rieu, M., and E. Perrier, Fractal models of fragmented and aggregated soils, in *Fractals in Soil Science*, edited by P. Baveye, J.-Y. Parlange, and B. A. Stewart, pp. 169–202, CRC Press, Boca Raton, Fla., 1998.

Rieu, M., and G. Sposito, Fractal fragmentation, soil porosity, and soil water properties, 1, Theory, *Soil Sci. Soc. Am. J.*, *55*, 1231–1238, 1991a.

Rieu, M., and G. Sposito, Fractal fragmentation, soil porosity, and soil water properties, 2, Applications, *Soil Sci. Soc. Am. J.*, *55*, 1239–1244, 1991b.

Rieu, M., and G. Sposito, The water characteristic curve of fragmented porous media and the fractal nature of soil structure, *C. R. Acad. Sci.*, *Ser. II*, *312*, 1483–1489, 1991c.

Stepanek, F., M. Marek, and P. M. Adler, Modeling capillary condensation hysteresis cycles in reconstructed porous media, *AIChE J.*, *45*, 1901–1912, 1999.

Sukop, M. C., G. J. van Dijk, E. Perfect, and W. K. P. van Loon, Percolation thresholds in 2-dimensional prefractal models of porous media, *Transp. Porous Media*, in press, 2001.

Tyler, S., and S. W. Wheatcraft, Fractal processes in soil water retention, *Water Resour. Res.*, *26*, 1047–1054, 1990.

N. R. Bird, Silsoe Research Institute, Wrest Park, Silsoe, Bedford MK45 4HS, England, UK. (nigel.bird@bbsrc.ac.uk)

E. Perfect, Department of Geological Sciences, University of Tennessee, Knoxville, TX 37996-1410, USA. (edp@yoda.gg.utk.edu)

M. C. Sukop, Department of Plants, Soils, and Biometeorology, Utah State University, Logan, Utah 84322-4820, USA. (msukop@mendel.usu.edu)

(Received November 14, 2000; revised May 25, 2001;
accepted May 31, 2001.)